NASA TECHNICAL MEMORANDUM

NASA TM X-53570

January 23, 1967

NASA TM X-53570

AN APPLICATION OF THE ELECTROMAGNETIC FLOWMETER FOR ANALYZING DYNAMIC FLOW OSCILLATIONS

By Houston M. Hammac
Propulsion and Vehicle Engineering Laboratory

NASA

George C. Marshall
Space Flight Center,
Huntsville, Alabama

TECHNICAL MEMORANDUM X-53570

AN APPLICATION OF THE ELECTROMAGNETIC FLOWMETER FOR ANALYZING DYNAMIC FLOW OSCILLATIONS

By

Houston M. Hammac

George C. Marshall Space Flight Center

Huntsville, Alabama

ABSTRACT

Development of an electromagnetic flowmeter (EMFM) of simple construction to study flow oscillations in turbopump systems is reported. The EMFM described was devised for measuring fluid flow fluctuations from an invariant state to 500 hertz without introducing any obstruction or disturbance to the dynamic transfer characteristics of the turbopump. The potential difference developed across the flowmeter electrodes was measured for fluid velocities ranging from approximately 20 centimeters per second to 1500 centimeters per second. The EMFM and associated electronic circuitry for detecting the flow signal resulted in a system capable of measuring fluid flow fluctuations over the entire design range for a period of three minutes with an accuracy of $\pm$ 2 percent.

NASA - GEORGE C. MARSHALL SPACE FLIGHT CENTER

NASA-GEORGE C. MARSHALL SPACE FLIGHT CENTER

TECHNICAL MEMORANDUM X-53570

AN APPLICATION OF THE ELECTROMAGNETIC FLOWMETER FOR ANALYZING DYNAMIC FLOW OSCILLATIONS

By

Houston M. Hammac

APPLIED MECHANICAL RESEARCH BRANCH
PROPULSION DIVISION
PROPULSION AND VEHICLE ENGINEERING LABORATORY
RESEARCH AND DEVELOPMENT OPERATIONS

TABLE OF CONTENTS

LIST OF ILLUSTRATIONS

LIST OF ILLUSTRATIONS (Concluded)

DEFINITION OF SYMBOLS

Symbol	Definition	Unit
A	Cross-sectional area normal to flow	$meter^2$
B	Magnetic flux density	$weber\text{-}meter^{-2}$
d	Diameter	meter
E_o	Measured output voltage	volt
e	Induced voltage	volt
g	Gap width	meter
H	Magnetic field intensity	$ampere\text{-}turn\text{-}meter^{-1}$
I	Current	ampere
J	Current density	$ampere\text{-}meter^{-2}$
ℓ	Length of path	meter
n	Number of turns	
Q	Volume of flow	$gallon\text{-}minute^{-1}$
R_i	Internal resistance	ohm
R_L	External load resistance	ohm
R_m	Resistance of flowing fluid media	ohm
V	Average velocity	$meter\text{-}second^{-1}$
α	Geometric weighting function	
μ	Magnetic coefficient	$henry\text{-}meter^{-1}$
μ_v	Space permeability of a vacuum	$henry\text{-}meter^{-1}$

DEFINITION OF SYMBOLS (Concluded)

Symbol	Definition	Unit
σ	Fluid or material conductivity	$mho\text{-}meter^{-1}$
ϕ	Lines of flux	weber
$\mathcal{M}$	Magnetomotance	ampere-turn
$\mathcal{R}$	Reluctance	$ampere\text{-}turn\text{-}weber^{-1}$
$\triangleq$	Is defined as	
$\approx$	Approximately equal to	
$\vec{E}$	Vector quantity	
$\oint$	Line integral	
$<<$	Much less than	

AN APPLICATION OF THE ELECTROMAGNETIC FLOWMETER FOR ANALYZING DYNAMIC FLOW OSCILLATIONS

By Houston M. Hammac
George C. Marshall Space Flight Center

SUMMARY

To study flow oscillations in turbopump systems, a flow transducer capable of accurately measuring high frequency flow variations is required. The flowmeter must not disturb or interfere with the dynamic transfer characteristics of the turbopump.

The electromagnetic and magnetoelectric flow transducers were investigated and compared as to advantages and disadvantages for selectivity. Performance of the electromagnetic flowmeter (EMFM) under steady fluid flow conditions is compared to that of a rotating turbine-type metering device. Principle of operation and theoretical and experimental design considerations are elaborated. Experimental data for fluid velocities ranging from approximately 20 cm/sec to 1500 cm/sec are included to illustrate the linearity and repeatability of the EMFM. Tap water was used as the fluid medium in the experiments. Application of the non-alternating flux EMFM provided fidelity in the measurements of flow oscillations. The non-alternating flux EMFM detects flow variations from zero up to ten kilohertz. However, it is limited to short-term data samples. Heat dissipation, electrode polarization and battery films obviate popular acceptance of the non-alternating flux EMFM.

INTRODUCTION

The concept of magnetic fluid flow measurement is dependent upon the Faraday Effect between the moving fluid and a magnetic field to produce an electrostatic potential proportional to the average flow velocity. This principle, in effect, states: "The voltage induced across any conductor as it moves through a magnetic field at right angles to the lines of flux, is proportional to the velocity of that conductor". This induced voltage vector will be at right angles to the magnetic lines of flux vector and the velocity vector of the conductor.

The field is expressed by the vector equation:

$$\vec{E} = \vec{V} \times \vec{B} \qquad (1)$$

where $\vec{E}$ is the electric field in volts per meter, $\vec{V}$ is the average velocity component of the fluid relative to the magnetic induction in meters per second and $\vec{B}$ is the intensity of the magnetic field in webers per meter squared. Figure 1 illustrates the essence of equation (1) as it pertains to magnetic flowmeters.

The electric field arises independently of the material content of the moving body, whether it be a conductor or a dielectric in the physical state of a solid, liquid or gas. Since the flowing medium in this application was tap water, the details of this discussion will be confined to a liquid conductor of low conductivity.

In open literature, it is often stated or implied that the output of a magnetic flow transducer is independent of the electrical conductivity of the fluid or gaseous media. There are certainly limitations to this statement. The electrical conductivity must not be so great that the magnetohydrodynamic forces will affect or distort the velocity profile, an effect that can occur with liquid metals. Also, there is a minimum conductivity (10^{-7} mhos per meter) below which the output characteristics of the magnetic flow transducer depends entirely upon the dielectric properties of the fluid media.

In the case of gaseous media, the output of the magnetic flow transducer is effectively zero, unless the gases are ionized. If the gases are ionized, an electrostatic potential will be created which is proportional to the flow velocity when it moves across a region of magnetic induction.

When dielectric fluids are to be metered by an electromagnetic device, the output is dependent upon induced polarization currents, and for this reason, a high frequency magnetic flux is usually employed, as the polarization currents induced in dielectric fluids are proportional to the frequency of induction.

If, however, the flowing medium is a conductor, induced conduction currents provide the signal power. Free charges are motivated under the influence of an electric field and produce a polarization in the body. This polarization is an electrostatic field and exists in both moving and stationary coordinate systems. Since the field is

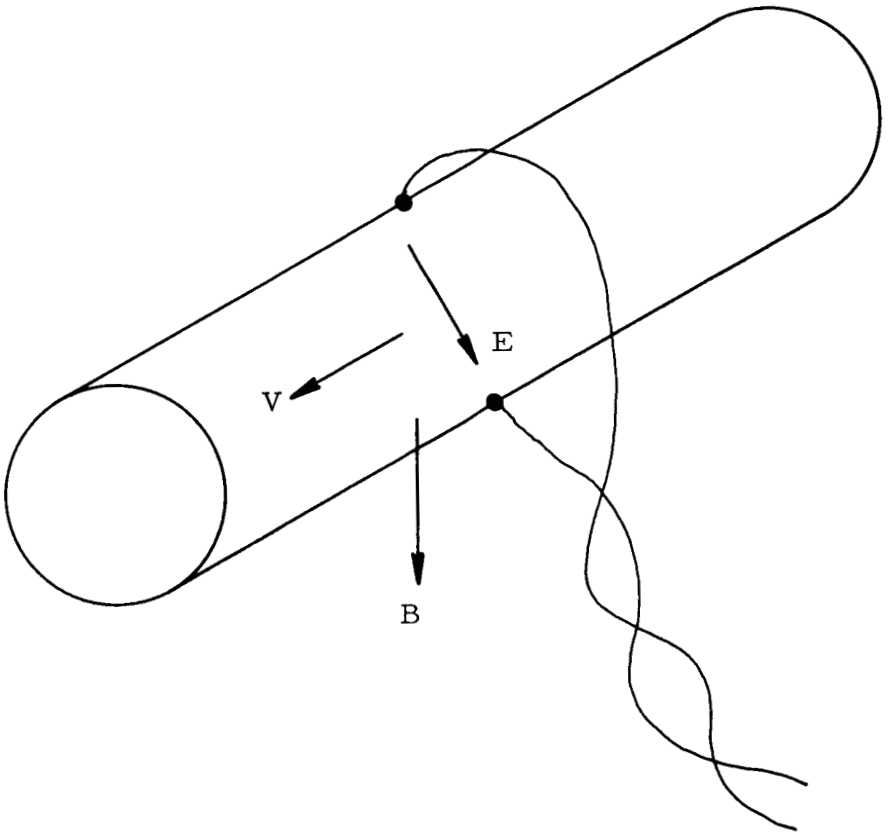

FIG. 1 SCHEMATIC REPRESENTATION OF MAGNETIC FLOW TRANSDUCER

electrostatic, it will give rise to a potential difference between a pair of electrodes, which in turn is electrostatic, and may be measured by conventional means in a stationary frame of reference.

EQUIVALENT CIRCUIT

To explicate the operation and the limitations of the magnetic flow transducer, equivalent circuits are shown in Figure 2 and are quantitatively resolved below.

An analysis of the circuit in Figure 2b yields a general expression for the measured voltage, i. e., the potential rise across the input resistance of the measuring instrument, R_L, as

$$E_o = \frac{V_{Bi}}{\left(1 + \frac{R_m}{R_s}\right)\left(1 + \frac{R_B}{R_L}\right) + \frac{R_m}{R_L}} \tag{2}$$

where: $R_m \triangleq$ flowing medium core resistance
$R_s \triangleq$ shunting resistance of flowing medium core due to end losses
$R_B = 2\,R_{bp} \triangleq$ probe boundary layer resistance
$R_L \triangleq$ input resistance of measuring instrument

The ratio R_m/R_s is a function only of the geometry associated with the physical construction of the magnetic metering device. Considering a constant value of R_L, the ratio R_B/R_L is a function of the hydrodynamic boundary layer thickness and possible other boundary layer parameters along with probe insertion depth. Also, if R_L is a fixed value, the ratio R_m/R_L is a function of the flowing medium conductivity.

By making the probes with a curvilinear surface area blending into the piping wall, the insertion depth is zero, and using a measuring instrument with a very large input resistance, $R_B \ll R_L$ and $R_m \ll R_L$ (which it would certainly be under normal conditions), Equation (2) reduces to:

$$E_o = \frac{V_{Bi}}{1 + \frac{R_m}{R_s}} \tag{3}$$

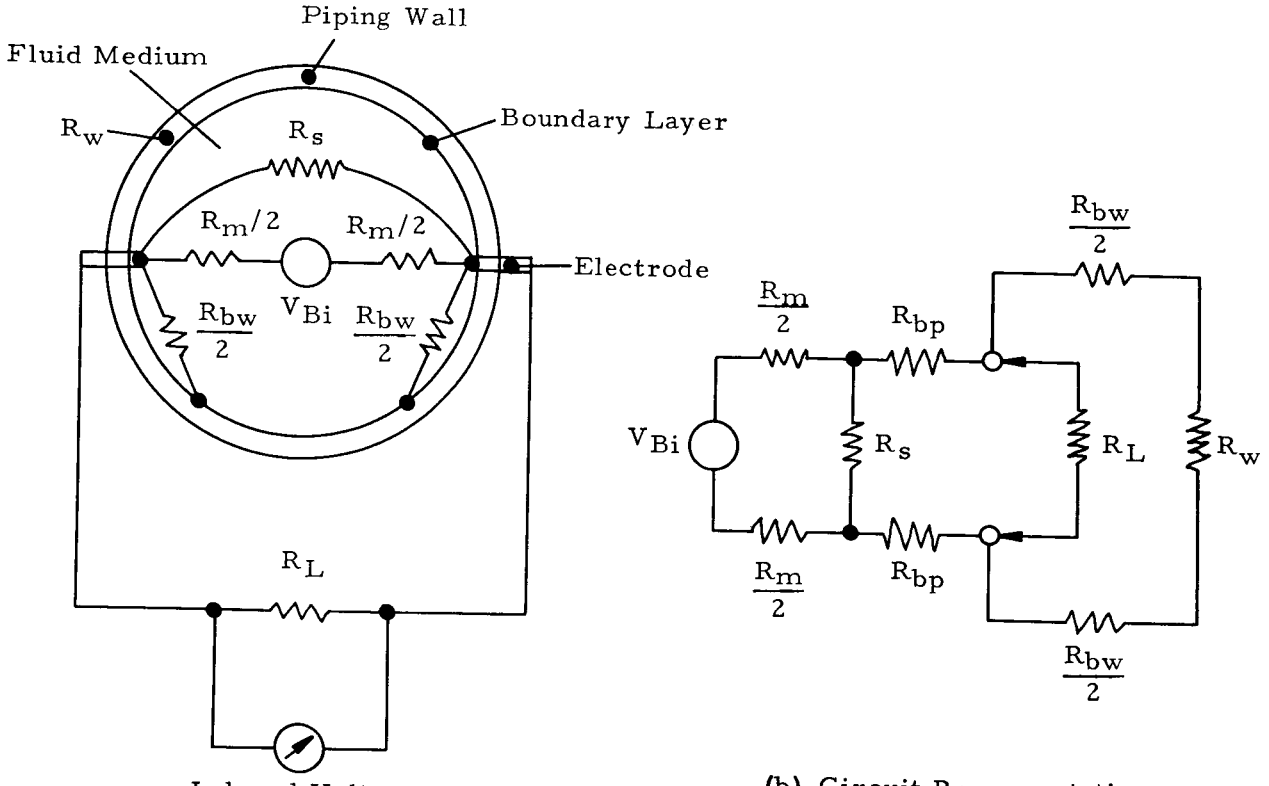

(a) Physical Representation

(b) Circuit Representation

V_{Bi} ≙ Electrostatic potential resulting from induced conduction currents by magnetic field

R_L ≙ External or load resistance

R_m ≙ Resistance of flowing media

R_s ≙ Shunting resistance due to end losses

R_{bp} ≙ Boundary layer resistance on probe

R_{bw} ≙ Boundary layer resistance on wall

R_w ≙ Resistance of the piping wall

FIG. 2 REPRESENTATION OF ELECTROMAGNETIC FLOW TRANSDUCER

Since R_m and R_s are of the same order of magnitude, E_o will have a value between $V_{Bi}/2$ and V_{Bi}. To determine the factor R_m/R_s more closely, the magnetic flowmeter must be experimentally calibrated.

Note that the terms R_w and R_{bw} have not been considered in the analysis of the magnetic flowmeter equivalent circuit. Thus, the expression for the electrostatic output potential developed across R_L does not reflect their presence. However, they are in parallel with R_L and it is imperative that the magnitude of the combination of R_w and R_{bw} be sufficiently large so as to minimize short-circuiting of the induced voltage in the section exposed to the magnetic field.

The equivalent circuits in Figure 2 hold true in their entirety only when a non-alternating magnetic flux is utilized. If an alternating current is used in an electromagnet to excite the magnetic induction, the stray capacitance that appears at the probes and at the input to the measuring instrument must be considered.

VELOCITY PROFILE

A potential, e, that is directly proportional to the average fluid flow velocity may be detected at the ends of a diameter that is perpendicular to both the flow velocity vector and the magnetic field vector provided the following conditions can be stipulated:

1. The fluid is flowing at a uniform velocity through a long, uniform and non-conducting pipe.
2. The magnetic flux is normal to the flow velocity vector.
3. The magnetic flux is uniform over the cross section of the pipe.
4. The magnetic flux is uniform over a length of pipe equidistant to several diameters.

Moveover, the potential varies as the average velocity varies. Therefore, a measurement of this existing potential postulates a measurement of the fluid flow velocity.

In a practical environment, the magnetic field is of limited extent and no potential will be induced outside the field. However, the fluid is conductive wherever it exists and end losses will tend to decrease

the voltage induced by the presence of the magnetic field. These end-shorting effects are alleviated by extending a non-magnetic flow tube approximately three diameters in each direction. This manipulation enables the magnetic field to be made sufficiently long that the shorting effects will be slight at the center of the lines of flux. Circulating current loops and end-shorting are illustrated in Figure 3.

Not only must the piping be non-magnetic, but in most applications it must be non-conductive so that the piping walls do not provide a short-circuit between the detecting electrodes. The degree of non-conductivity is dependent upon the conductivity of the flowing media. As the conductivity of the flowing medium decreases, the non-conductivity of the piping walls must increase. There must be no amperian current flow from the fluid into the tube walls or measuring circuitry. If these restrictions are relaxed, circulating currents occur within the fluid and introduce ohmic losses. The presence of conducting walls can reduce the output potential to zero unless the fluid conductivity is greater than the wall conductivity. In practice it is not feasible to construct an entire piping installation of non-conductive material, therefore, a compromise is instituted where only the necessary three diameters in each direction are composed of non-conductive piping.

Although it was stipulated that the velocity profile be uniform, in actual practice flows are never of this precise form. If the flow is turbulent, however, the results expressed previously are still valid, so long as the flow is symmetric about the axis. Figure 4 portrays the symmetrical potential distribution resulting from axial fluid flow symmetry.

Should the flow not be symmetric about the pipe axis, the integral of the local velocity times a weighting function must be considered. This will yield an indication of the ability of the flow at various points to contribute to the induced potential.

SIGNIFICANCE OF CALIBRATION

The need for calibrating the EMFM is best explained by considering the previously mentioned geometric factor, R_m/R_s. Theoretically, the induced voltage, e, and the resulting output potential, E_o, could be calculated for an ideal magnetic flowmeter from the relationship

$$e = B\ell V \qquad (4)$$

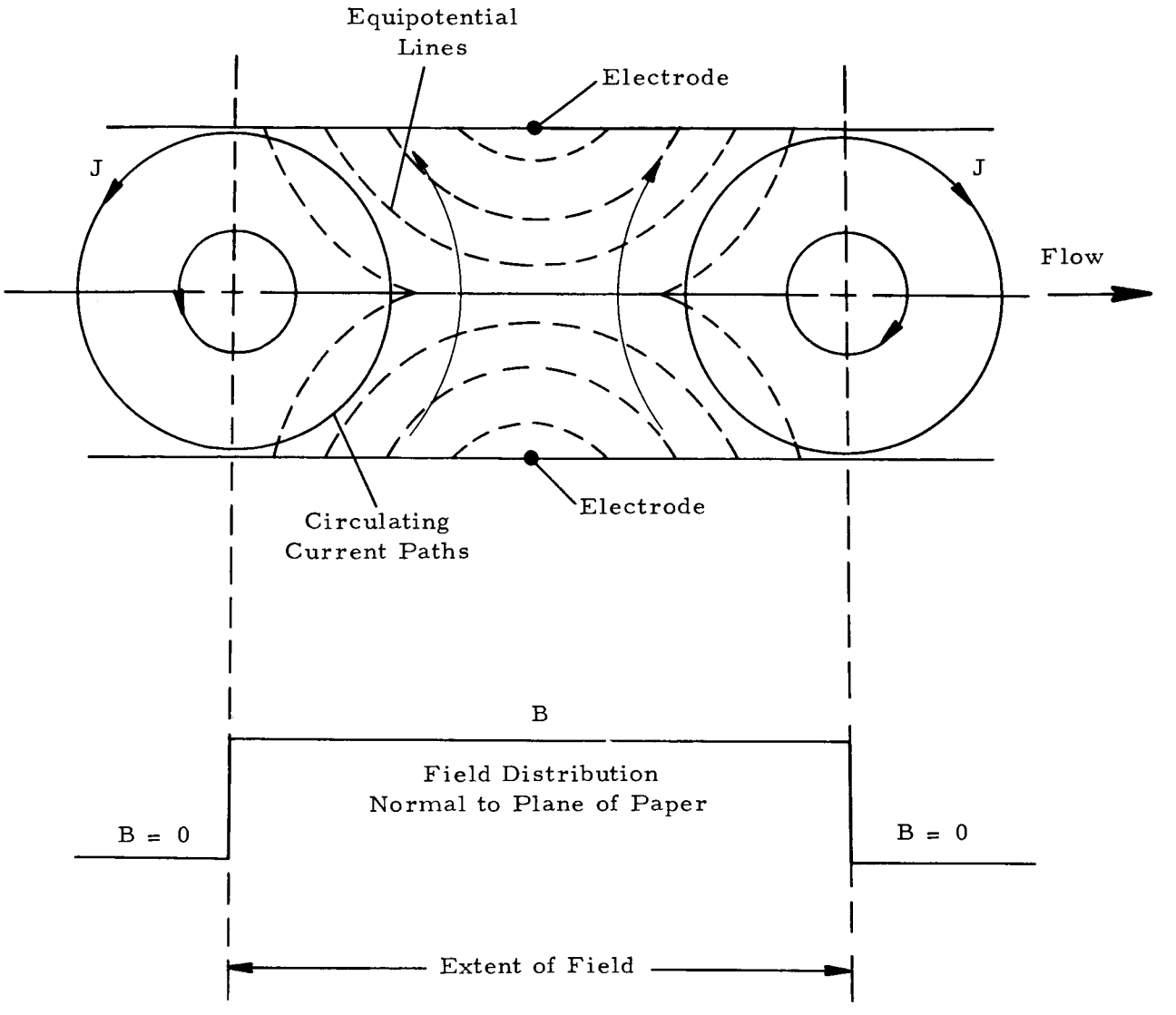

FIG. 3 SCHEMATIC ILLUSTRATION OF CIRCULATING CURRENT LOOPS AND END-SHORTING

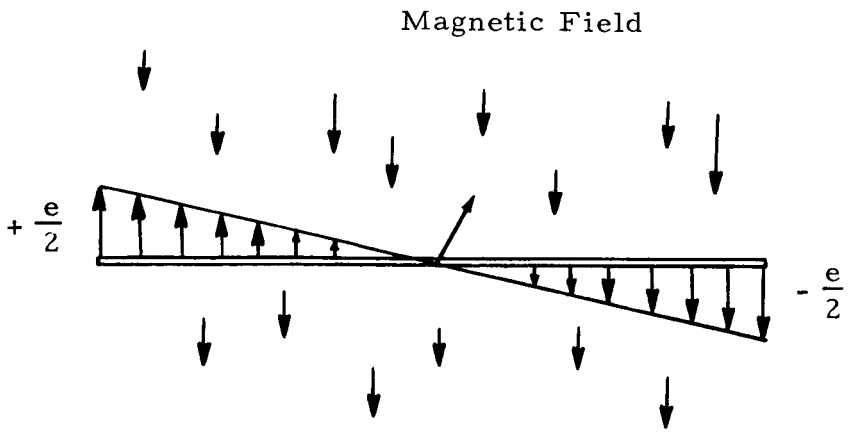

(a) Transverse Plane

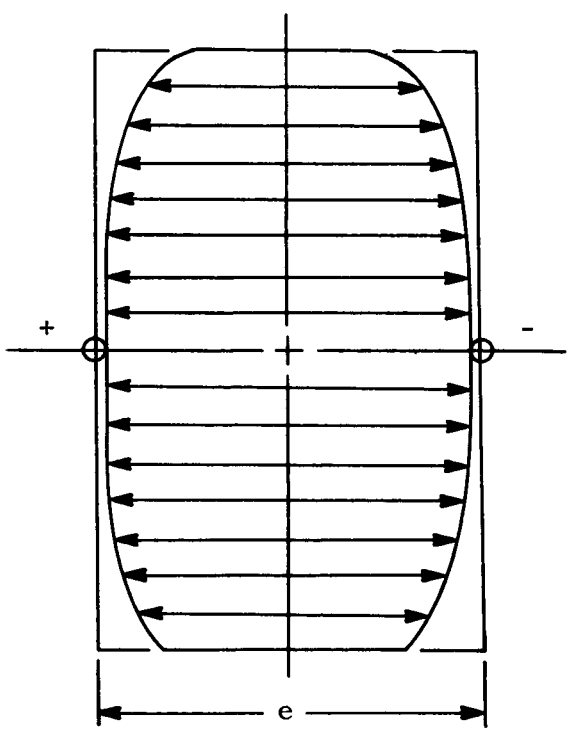

(b) Axial Plane

FIG. 4 SYMMETRICAL POTENTIAL DISTRIBUTION

where: $\ell \triangleq$ length of the conductor in meters
$V \triangleq$ average velocity of the conductor in meters per second

In the magnetic flowmeter, ℓ is the distance between the electrodes or, in the case of flush mounted curvilinear electrodes, the inside diameter of the piping wall.

In practical applications, however, equation (4) must be modified and a better approximation is

$$E_o = \alpha B \ell V \tag{5}$$

where α is a geometric constant for a given flowmeter that takes into account end losses.

In terms of feasibility, equation (5) will not predict the output of every magnetic flowmeter with a single value of alpha. Since the constant, α, is geometrically dependent, and an alteration in flowmeter design will change the slope of the experimental calibration curve, each magnetic flowmeter will need an individual experimental calibration. However, the calibration is linear and is valid for other flowing media of different electrical conductivities and densities without application of any peculiar correction factors.

FLOWMETER SELECTION

A system was designed to study flow oscillations and dynamic transfer characteristics of a turbopump. The physical structure of the system established some stringent and demanding requirements of the flow measuring device. To match the outlet of the pump, the inside diameter of the flowmeter tube had to be 3.8 centimeters. The flowmeter, located between the pump outlet and a flow pulsing device, could not offer any obstruction or disturbance to the flow. Detection of flow variations up to 500 hertz was required. This was later relaxed to 100 hertz. Another important requirement was that the transducer be simply constructed and compatible with standard instrumentation electronics.

In consideration of the above demands, a magnetic flowmeter with a non-alternating induction flux was selected, because its frequency response ranges from zero to approximately ten kilohertz. An alternating induction flux has its upper frequency response bounded by the frequency of the flux employed. The frequency of the alternating flux must be much greater than the highest flow fluctuation to be detected.

Piping Material

Plexiglass, a member of the acrylic polymer family with a conductivity of less than 0.1 picomhos per meter, was selected for the flow-tube portion of the flowmeter. Since tap water has a conductivity of approximately 20 millimhos per meter, the ratio of the conductivities indicate that Plexiglass will exhibit negligible shorting between the detection electrodes. Stainless steel, being essentially non-magnetic, was utilized to construct a connection framework for installing the flowmeter in the pumping system.

Detection Electrodes

The conductivity of the flowing medium becomes a limitation of the non-switching flux type EMFM. Fluid conductivity must be sufficiently large so that the internal resistance of the induced voltage source is small compared with the input impedance of the external detection instrument. Otherwise, excessive loading of the induced voltage source will occur. The internal resistance of the induced voltage source is the resistance between the detection electrodes. From theory, the internal resistance is approximated by

$$R_i \approx \frac{1}{\sigma d_e} \tag{6}$$

where: $\sigma \triangleq$ fluid conductivity in mhos per meter
$d_e \triangleq$ detecting electrode diameter in meters

From expression (6), it is evident that to decrease the internal resistance the electrode diameter must be made large. As is true in most physical applications, a compromise must be conceded. If the electrodes are made too large in diameter, they become impractical; if their diameter is made too small, the induced signal will be attenuated. Based upon calculations by Balling and Conner [1], one millimeter is the minimum electrode diameter that will not excessively attenuate the induced signal. To avoid the possibility of signal attenuation and maintain feasible size, a diameter of 9.5 millimeters was chosen. This yields an internal resistance for the induced

voltage source of about 5200 ohms. Mild steel screw stock was procured and machined, and the finished product gold plated to prevent rust and corrosion.

Magnetic Flux Generator

An electromagnet was chosen to generate the magnetic flux, primarily because its field strength could be readily adjusted by increasing or decreasing the number of turns of wire wound on the core and the amount of excitation current supplied by the power supply. Moverover, a permanent magnet with a 4.7-centimeters air gap was not readily available.

A suitable core was contrived from the double "E" core of a power transformer, and pole faces were acquired from a direct current motor. The resulting "C" core is illustrated in Figure 5.

Realizing that the excitation current would by necessity have to be large, 14 AWG gauge magnet wire was selected to form the electromagnet.

Figure 6 is an artist's conception of the finished product minus the tube mounting connections.

FUNCTIONAL TESTING

The completed electromagnetic flowmeter was installed in the experimental facility for calibration. To acquire a steady-state calibration, a turbine-type flowmeter was selected as the most readily available means of comparison.

Difficulties were encountered from the outset. It was quickly recognized that an output existed when the piping was filled with water, even without flow or magnetic flux present. To further complicate the situation, the output exhibited a low frequency random drift. Using an oscilloscope with a high gain differential plug-in unit possessing an input impedance of one megohm, measurements were obtained to determine the nature of this phenomenon. Figure 7 illustrates the potentials that existed during one set of measurements. The potentials shown are not necessarily the largest nor the least found to be present. Also, a dramatic change ("flushing" effect) in the magnitudes occurred

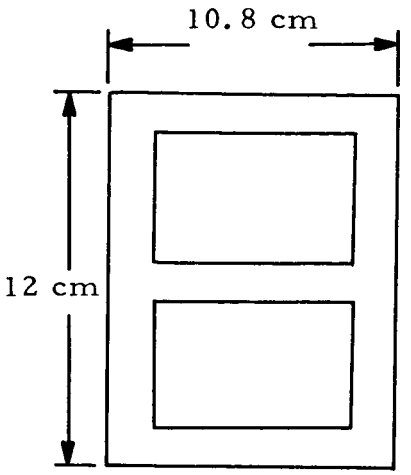

(a) Transformer Double "E" Core

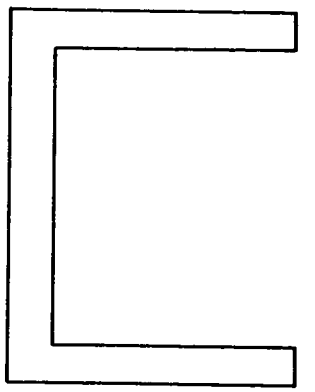

(b)

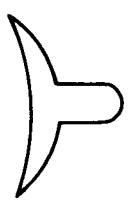

(c) Motor Pole Face

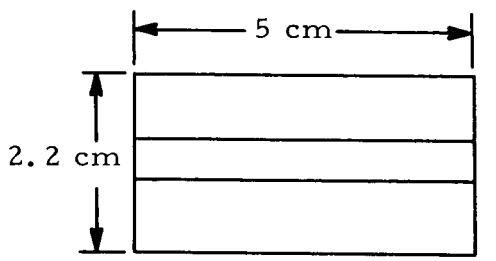

(d)

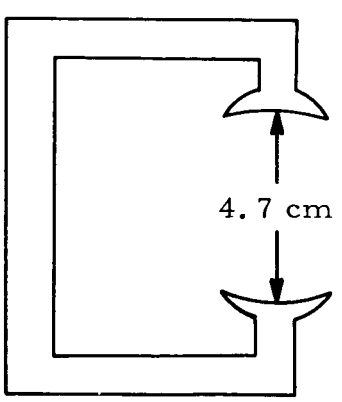

(e)

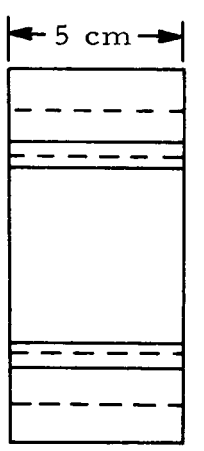

(f)

FIG. 5 CONTRIVED "C" CORE USED IN FORMING ELECTROMAGNET

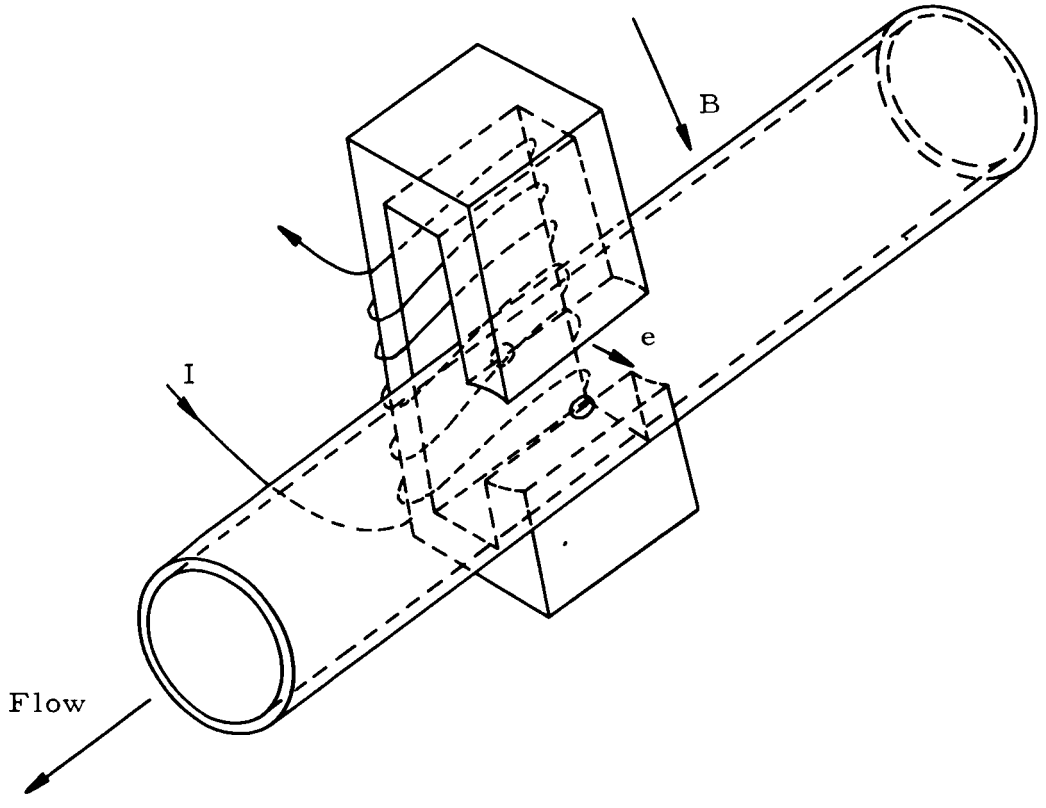

FIG. 6 A PICTORIAL REPRESENTATION OF THE COMPLETED ELECTROMAGNETIC FLOW METER EXCLUDING THE TUBING CONNECTION HOLDING FRAME

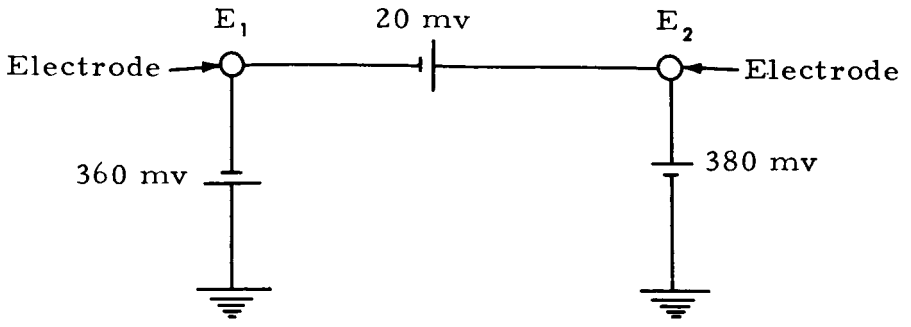

(a) Non-flowing Fluid

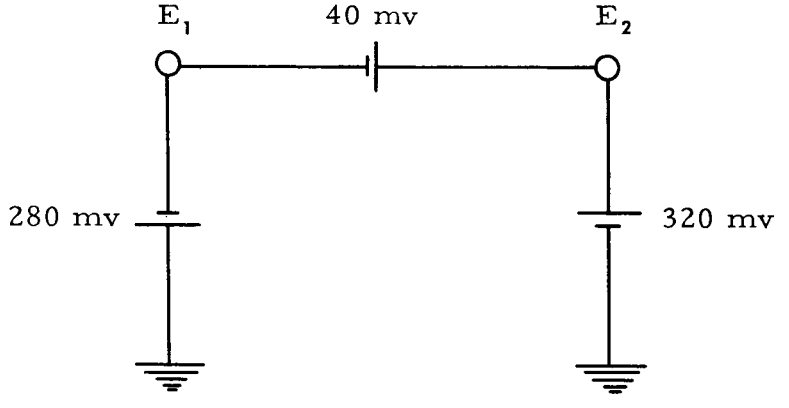

(b) Flowing Fluid

FIG. 7 TYPICAL POTENTIALS EXISTING BETWEEN ELECTRODES AND BETWEEN ELECTRODES AND GROUND

if fluid flow was introduced. As the investigation progressed, measurements revealed that the polarties shown in Figure 7 did not persist. Over a period of several days, the electrodes changed polarities with respect to each other. During that time another phenomenon occurred; long-term immersion of the electrodes reduced the potentials in Figure 7, and the frequency of variation decreased. The magnitude of the variation decreased and the drastic change that had taken place previously between flowing and non-flowing conditions was not now so extreme in effect.

Since the potential difference that existed between the apparently identical electrodes was of the same order of magnitude as the induced signal, efforts were directed toward elimination or alleviation of the effects of its presence. The identicalness of the electrodes not being certain, cathodic evolution of hydrogen and anodic evolution of oxygen seemed to be the most logical explanation for the electrode reactions. Evidently, to deter the presence of any electrochemical potentials, the purity of the material from which electrodes originate is of the utmost importance.

New electrodes were machined from a 300 series stainless steel. When using the stainless steel electrodes, the potentials in Figure 7 were on the order of one-tenth the magnitude shown. Moreover, the magnitude and frequency of drift was much less than before. Another marked improvement was the smaller "flushing" effect when fluid flow was introduced. However, the stainless steel electrodes did not perform satisfactorily when the magnetic flux was switched on and off. A polarization was induced in one direction when the flux was switched on and in the reverse direction when the flux was switched off. The polarization induced by the magnetic flux being switched off was inherently slow returning to its original value. The same sluggishness also prevailed in the reverse situation. It was difficult to distinguish between the polarization drift towards its original level and the random drift or a slight variation in flow. The stainless steel electrodes were therefore discarded.

Other investigations suggested that platinum electrodes yield better results than electrodes constructed from other materials. The only platinum available was 0.8 millimeter diameter wire. Electrodes were made of it, but the induced signal was attenuated because the diameter of the wire was too small. Moreover, the platinum possessed characteristics similar to the stainless steel electrodes, but not as detrimental.

Because of the above, attention returned to the original electrodes. By allowing the fluid flow to be present for ten to fifteen minutes, the existing potential became fairly steady. The amount of time required to attain this condition depended upon the length of time that the fluid flow had been off. However, after the semi-steady potential condition had been realized, short interruptions in flow had little effect on the electrochemical potential.

The windings of the electromagnetic flowmeter dissipated heat to the extent that it could not be left energized for extended periods of time. The time could be increased by using forced air cooling, decreased excitation current, or both. The heat dissipated by the electromagnet made the magnetoelectric flowmeter seem more advantageous. However, since the magnetic flux of the permanent magnet could not be interrupted, output change due to fluid flow and the "flushing" effect were inseparable. Hence, the magnetoelectric flowmeter was reprobated for the application at hand, but this should not be construed to mean that it is not feasible. For an application in which measurement of dynamic fluctuations of fluid flow will suffice, capacitive coupling may be employed to allow mensurations from approximately one hertz to ten kilohertz.

A turbine-type flowmeter was installed in the system to calibrate the EMFM. A differential voltmeter with an input resistance of one megohm was used to detect the induced potential of the EMFM. The relationship established between fluid flow and EMFM millivolt output is presented in Figure 8. The calibrated EMFM was incorporated into a measuring system. A differential direct current amplifier with a one megohm input resistance, containing a 100 hertz cut-off filter, was selected as the active signal conditioner. Since the objectionable potentials present were of the same order of magnitude as the desirable signal, the undesirable signal had to be minimized prior to amplification. The circuit in Figure 9 shows by what means this was accomplished. Bucking voltage was supplied by a nickel-cadmium battery, which provides a very stable voltage. A reversing switch is provided for coping with sometimes transposing electrodes. Prior to each test, the potentiometer was used to null the input to the amplifier.

After the initial calibration, test requirements were increased from a nominal 110 gal/min to 200 gal/min. Thus, a subsequent calibration yielded the relationship in Figure 10. Examination of the higher flowrates revealed that the inherent linearity seemed to be awry; however, further investigation revealed that the gold-plating on

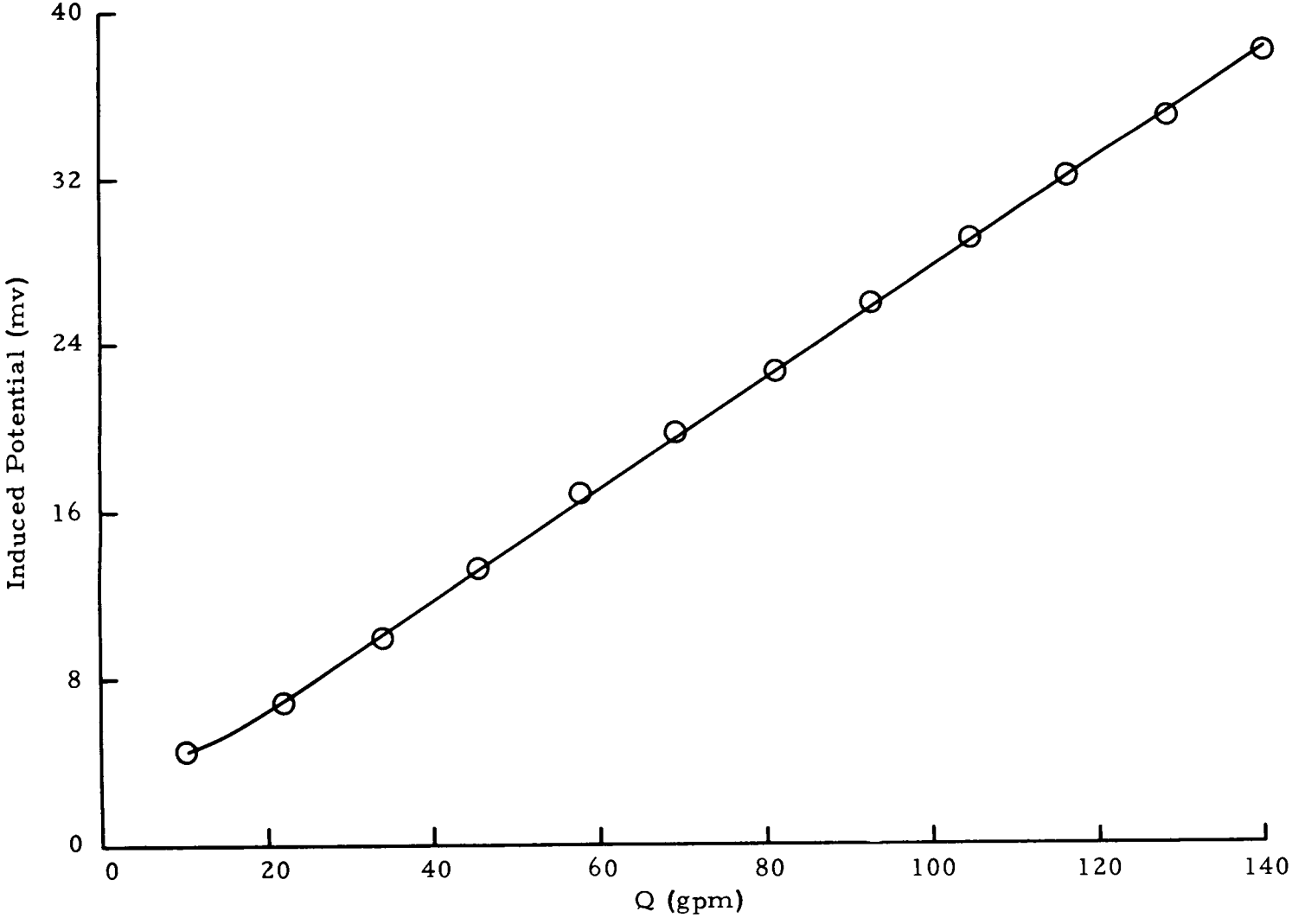

FIG. 8 EMFM OUTPUT VERSUS FLUID FLOW (0 - 110 gpm) UTILIZING MILD STEEL GOLD-PLATED DETECTION ELECTRODES

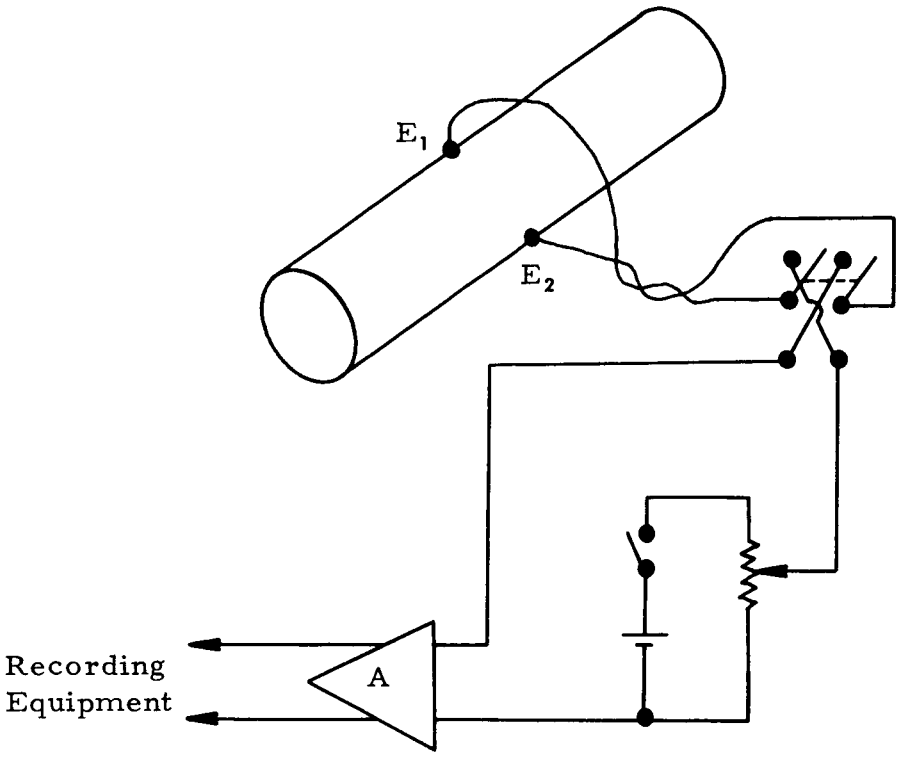

FIG. 9 METHOD OF ELIMINATING BULK OF UNDESIRABLE POTENTIAL

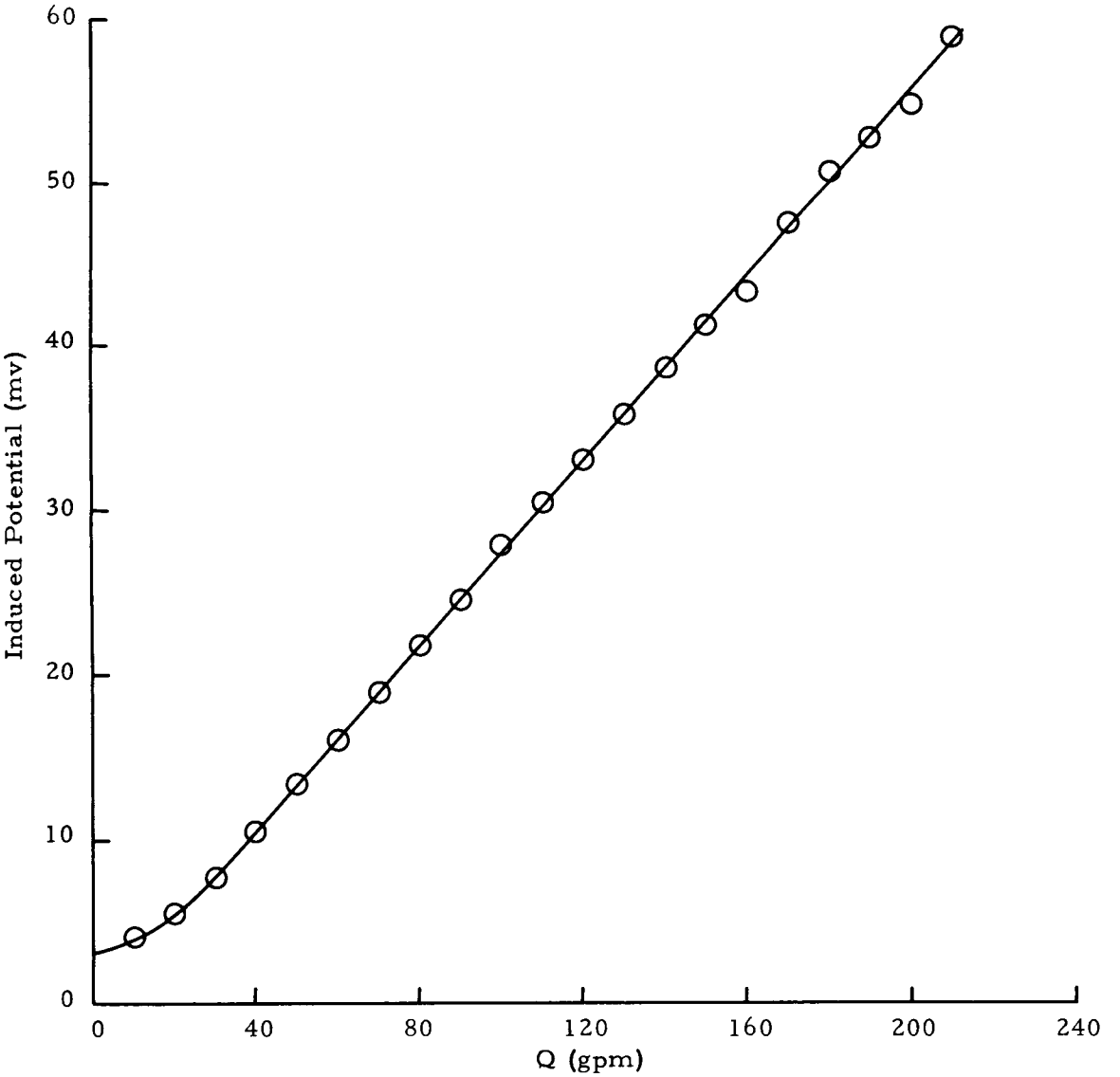

FIG. 10 EMFM OUTPUT VERSUS FLUID FLOW (0 - 200 gpm) UTILIZING MILD STEEL GOLD-PLATED DETECTION ELECTRODES

the electrodes had not remained intact and had started to pit. Figure 11 illustrates a calibration of the same electrodes with even more severe pitting. Pitting in the electrodes produced a very unstable and extremely noisy signal, attesting to the fact that the electrodes must be highly polished on all the surface area exposed to dynamic flow conditions for optimum results.

It was evident that new electrodes had to be acquired with a longer life expectancy while maintaining the desirable characteristics of mild steel. Moreover, time was of the essence and would not permit a long delay in obtaining material.

Satisfactory results were obtained from electrodes contrived from gold-plated silver relay contacts. The new electrodes had a smooth polished surface, but did not possess a curvilinear flush mounting configuration in the flowmeter wall. Hence, some disturbance to fluid flow would be induced by the 1.5 millimeters protrusion of the electrodes. The influence of the protrusion on the final results was determined to be negligible. This conclusion was validated by comparing data obtained with the curvilinear electrodes and the new protruding electrodes. Disturbance introduced by the protruding electrodes was not discernible, because enormous amounts of disturbance were already present from other sources in the system. The performance of the new electrodes was very good during the on and off switching of the magnetic flux. The polarization potentials were essentially unchanged from that of the mild steel gold-plated electrodes.

A calibration curve for the latest configuration of detection electrodes is displayed in Figure 12. The curve indicates that a larger potential is developed at the new detection electrodes than was previously available at the mild steel electrodes. Such is not the case, however, and the difference is accounted for by considering the input impedance of the detecting instruments. The data in Figure 12 were obtained using an instrument with an input impedance of ten megohms. The non-linearity at the low end of the calibrations connotes a departure from theory. Exact slopes and terminations were not obtainable due to the inability of the turbine meter to perform at the low flowrates.

Behavior of various detection electrodes under the influence of magnetic flux being switched on is depicted in Figure 13. The illustrated behavior is also typical of the action that occurs when the magnetic flux is switched off. Experimental data collected were satisfactory in both consistency and repeatability. Figures 14 and 15 show the equipment used to perform the experimental portion of this development project. Figure 16 shows the curvilinear flush mounting detection electrodes.

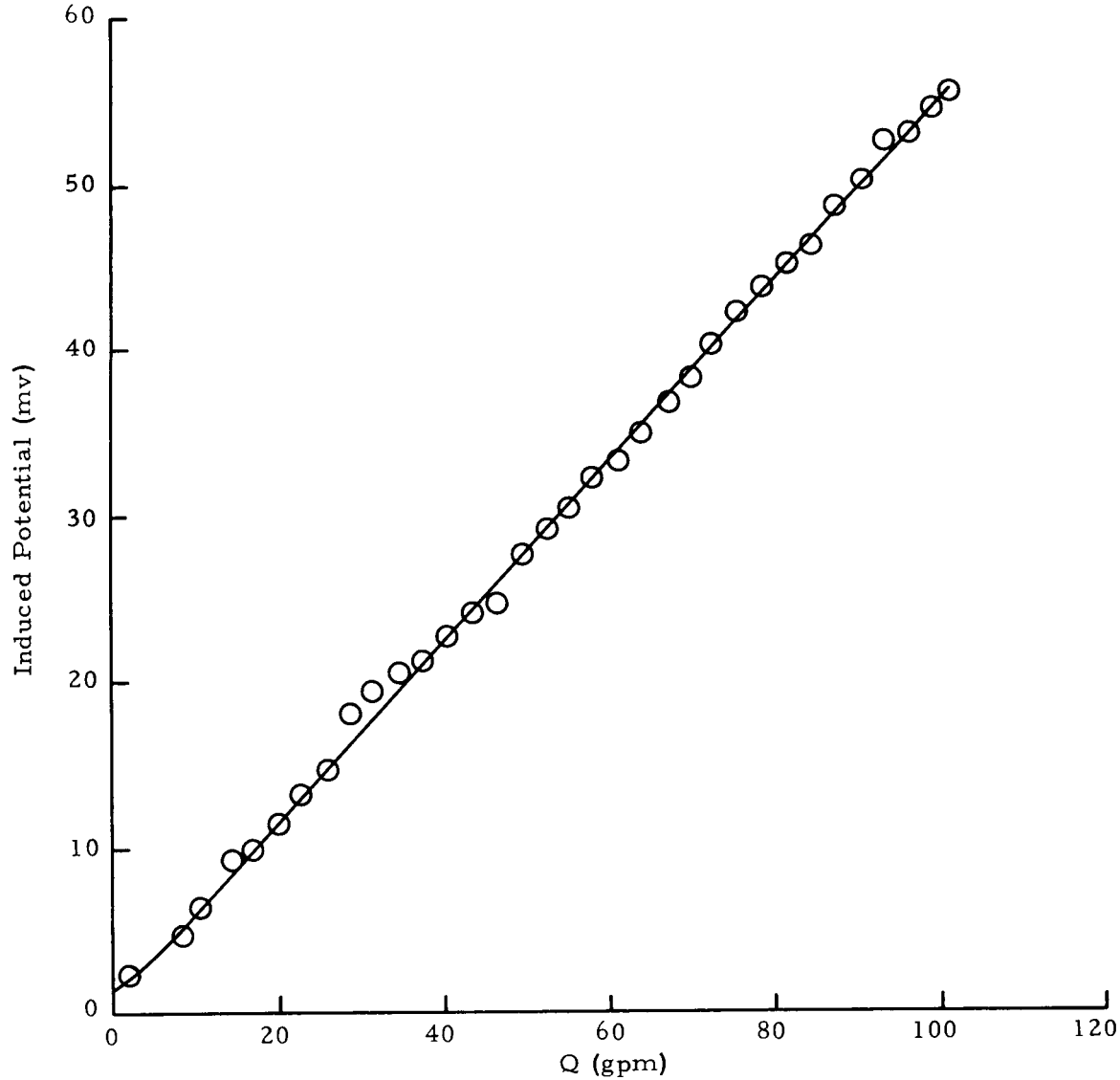

FIG. 11 EMFM OUTPUT VERSUS FLUID FLOW UTILIZING MILD STEEL GOLD-PLATED DETECTION ELECTRODES (PITTED ELECTRODES)

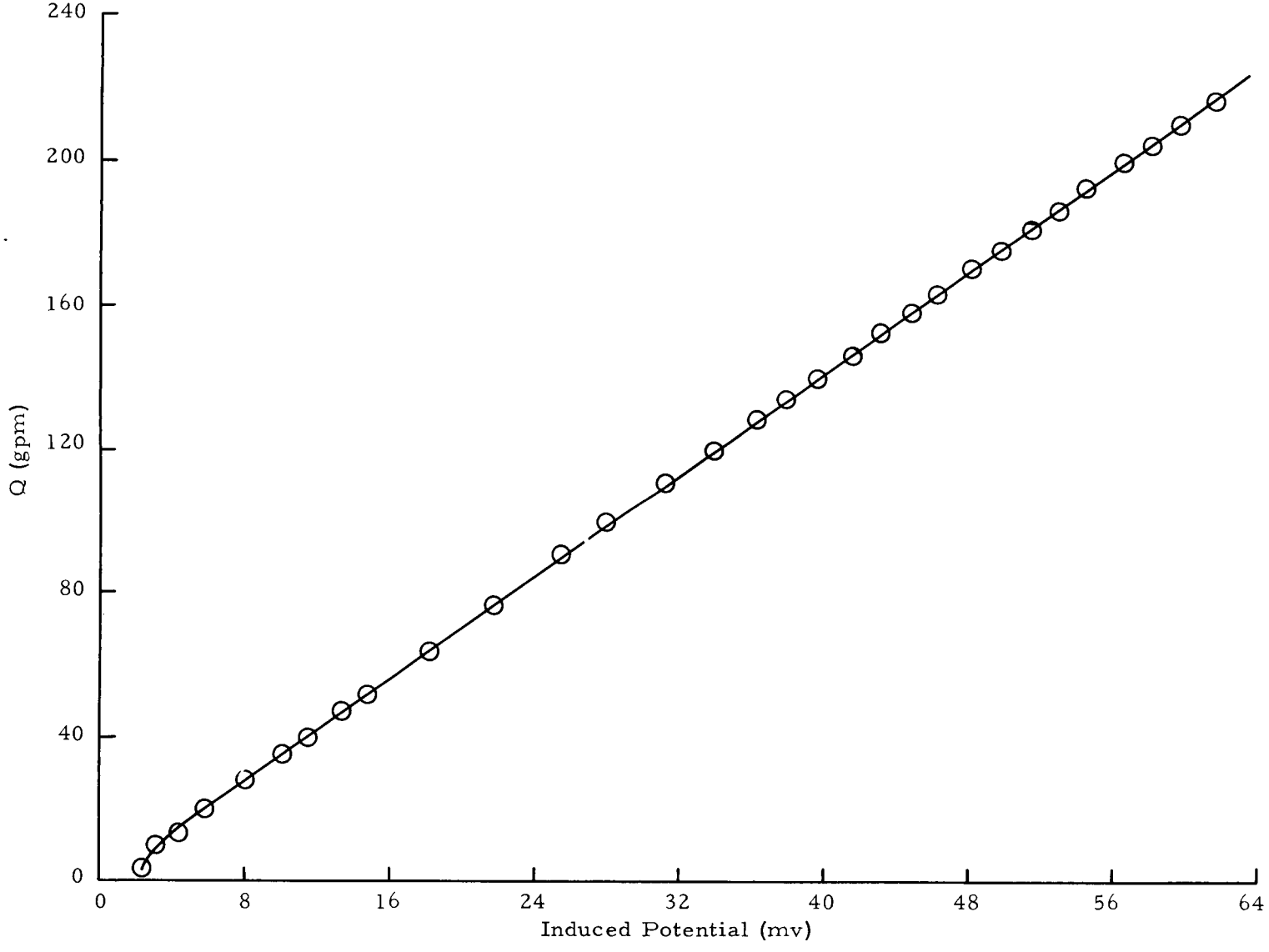

FIG. 12 EMFM OUTPUT VERSUS FLUID FLOW UTILIZING GOLD-PLATED SILVER DETECTION ELECTRODES

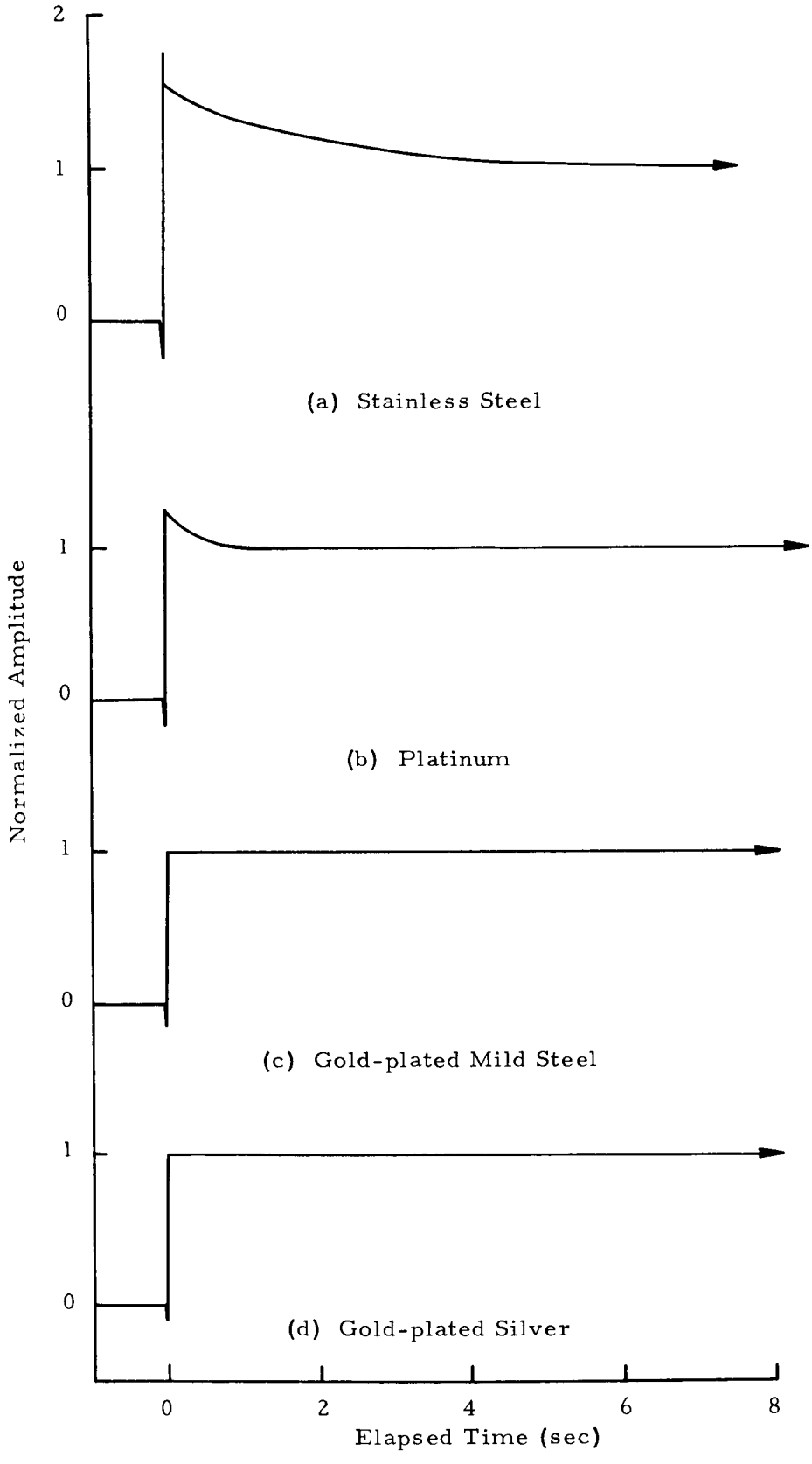

FIG. 13 COMPARISON OF ELECTRODES UNDER INFLUENCE OF MAGNETIC FLUX BEING SWITCHED ON

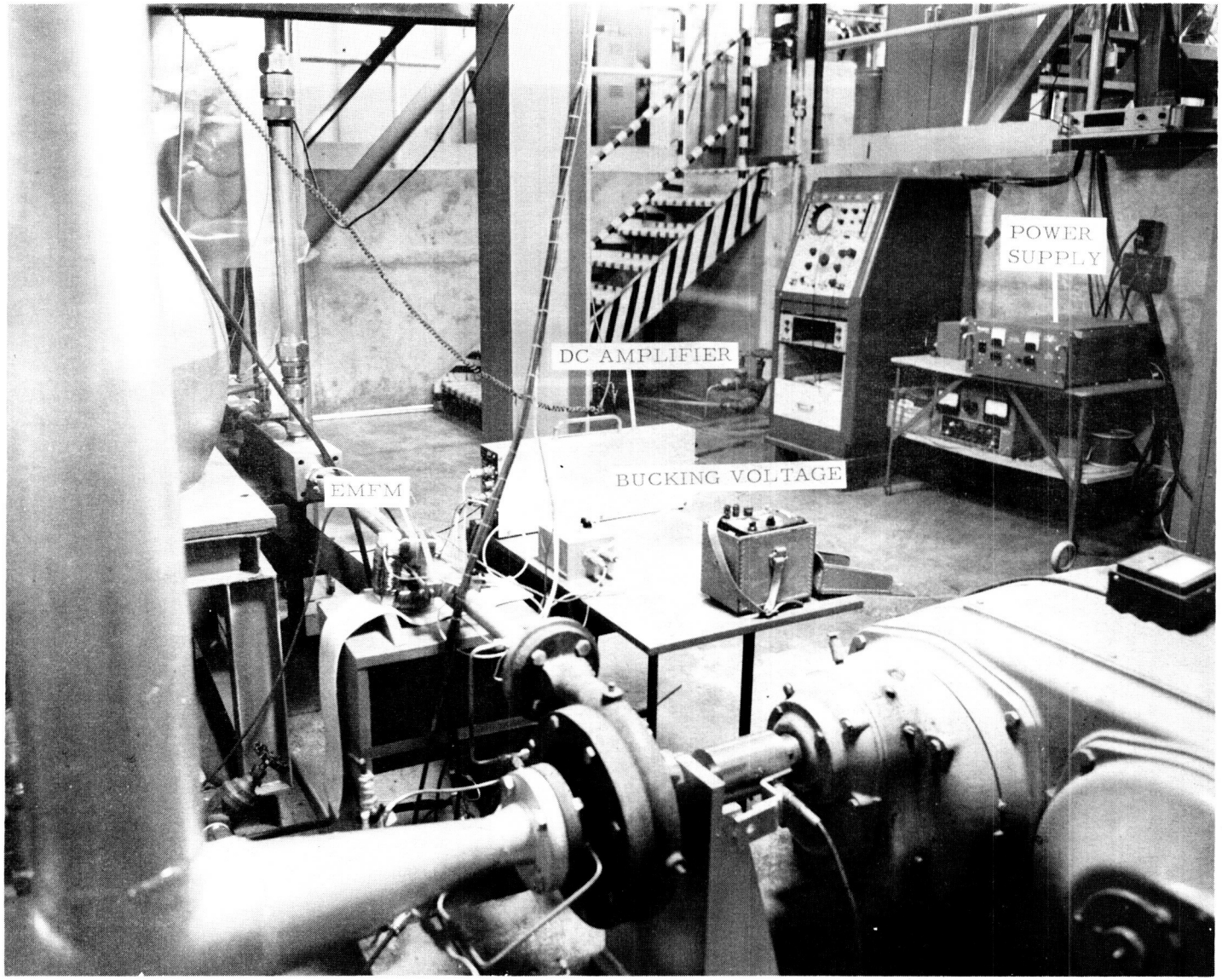

FIG. 14 EXPERIMENTAL TEST APPARATUS

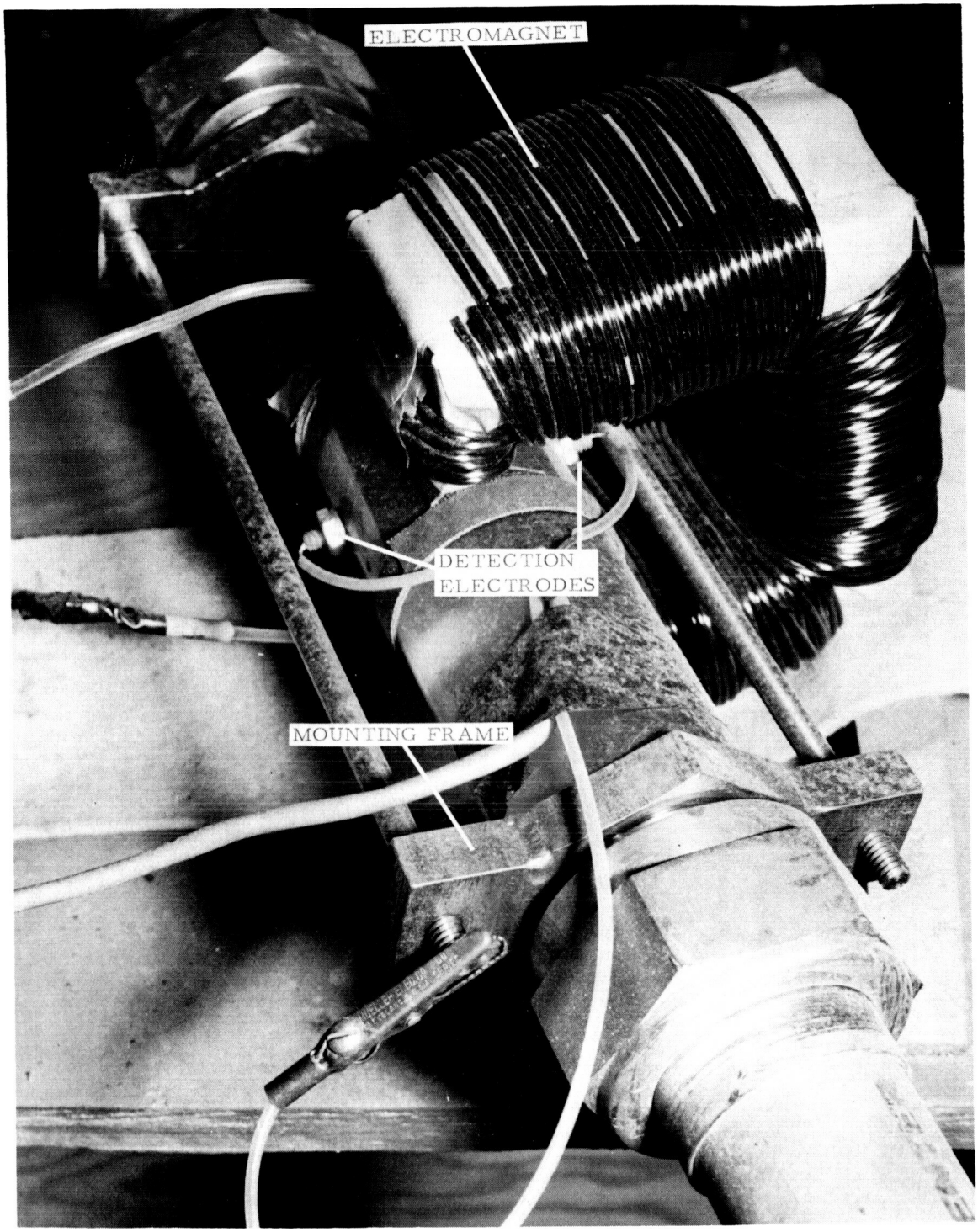

FIG. 15 COMPLETED ELECTROMAGNETIC FLOWMETER INSTALLED IN EXPERIMENTAL APPARATUS

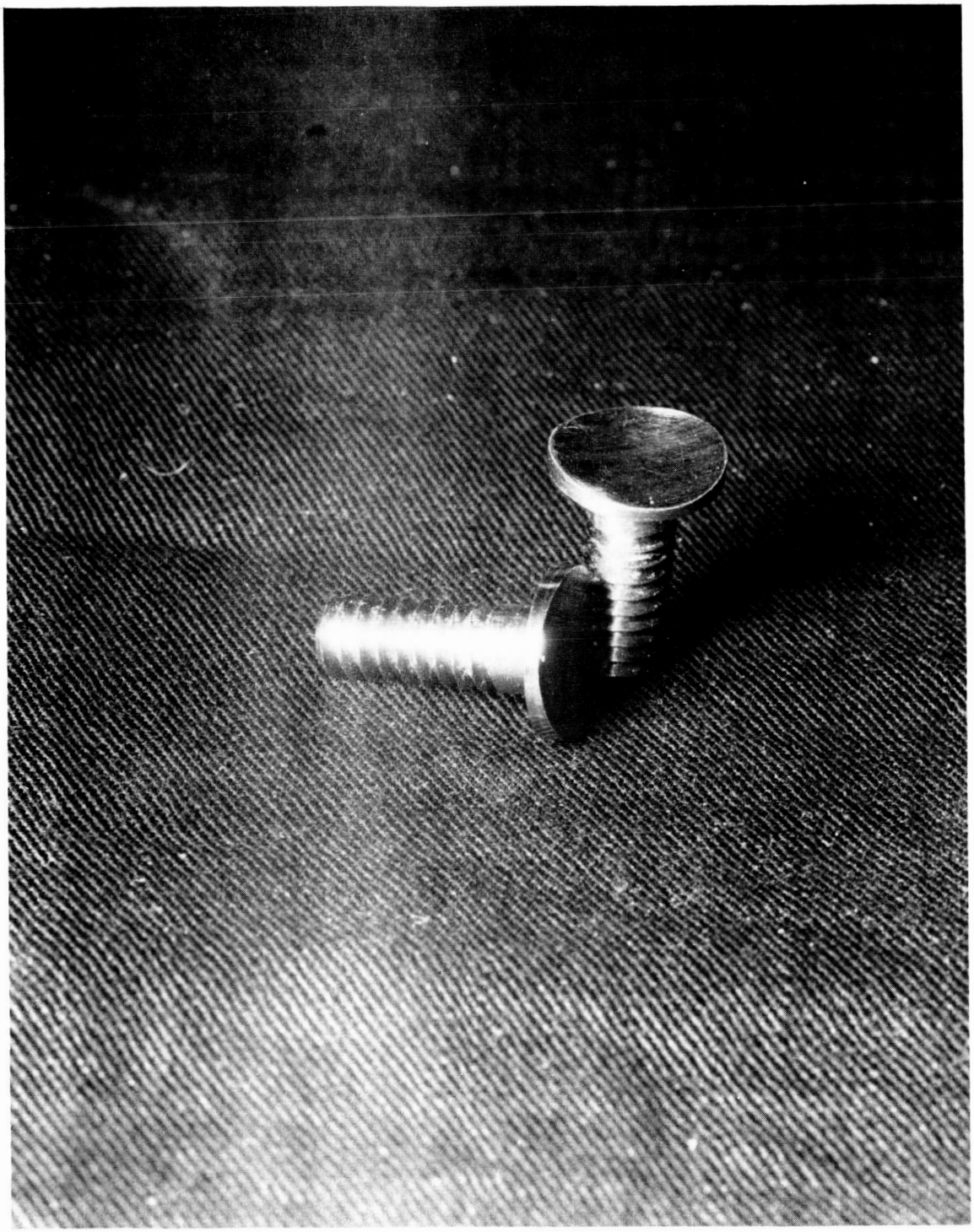

FIG. 16 CURVILINEAR FLUSH MOUNTING DETECTION ELECTRODES

CONCLUSIONS

Conclusions to be formed from the experiments are numerous. One can certainly visualize the vast applications for a flow transducing device offering an obstructionless path to flow and extremely high frequency response. Moreover, flow ratios of 200 to 1 are within the realm of possibility. However, the perplexing peculiarities inherent in the simplest form of the magnetic flowmeter cannot be ignored.

Even though it has proven to be a very useful transducer for short-term mean-valued flow fluctuations, the desire to provide accurate long-term flow rates must be acknowledged. The slowly varying polarization potential present at the detection electrodes discourages frequent application of the non-alternating flux variety of magnetic flowmeter to the measurement of flows in low-conductivity fluids. However, the variation and magnitude of the slowly varying polarization potential can be greatly minimized by selecting detection electrodes with low impurity content, by long term soaking in the fluid medium, and by the biasing technique introduced by E. G. Laue [2]. The electrodes must be highly polished on all surfaces exposed to the fluid medium to acquire the optimum in a noise free signal.

An alternate method of utilizing the non-alternating flux electromagnetic flowmeter involves a "zero-check" technique. The frequency of zero-check is one of arbitrary selection. Once every thirty seconds will provide sufficient lengths of continuous data for most applications. The zero-check is made possible by the capability to interrupt the excitation current of the electromagnet. By periodically sampling the zero, a new reference is obtained for each subsequent test excerpt. By employing this technique, more accurate and meaningful data can be obtained over longer periods of time than previously proclaimed.

The outstanding characteristic of the magnetic flowmeter is that, since it is basically a velocity meter and behavior is virtually independent of fluid conductivities, it can be calibrated with one fluid medium and employed with other media without recalibration or compensation techniques, provided the aforementioned loading and shunting effects are not limiting factors.

APPENDIX

The maximum number of turns of 14 AWG gauge wire that could be wound onto the "C" core was 489 turns. Since most of the magnetomotance of the exciting coil is required to force the lines of flux across the air gap, reluctance drop in the metal portion of the core can be ignored in calculating the magnetic flux density.

To justify this assumption, refer to Figure 17. The closed path of the magnetic flux is the length, ℓ, of the metal and gap width, g. The reluctance of the metal core is then

$$\mathcal{R}_e = \frac{l}{\mu_m \mu_v A} \quad \text{ampere-turns per weber} \qquad (7)$$

where: $\mu_v \triangleq$ space permeability of a vacuum
$\mu_m \triangleq$ relative permeability of material
$A \triangleq$ cross-sectional area in meters squared

Similary, the reluctance of the gap is

$$\mathcal{R}_g = \frac{g}{\mu_a \mu_v A} \quad \text{ampere-turns per weber} \qquad (8)$$

Reluctances in a magnetic circuit are combined in the same manner as resistances in an electric circuit. Therefore, the total reluctance of the magnetic circuit in Figure 17 is determined by summing equations (7) and (8).

$$\mathcal{R} = \frac{l}{\mu_m \mu_v A} + \frac{g}{\mu_a \mu_v A} \quad \text{ampere-turns per weber} \qquad (9)$$

In most engineering computations, the permeability of air is arbitrarily taken as unity, and the permeability of soft iron is about 5000. Therefore, equation (9) reduces to the expression

$$\mathcal{R} \approx \frac{g}{\mu_v A} \quad \text{ampere-turns per weber}$$

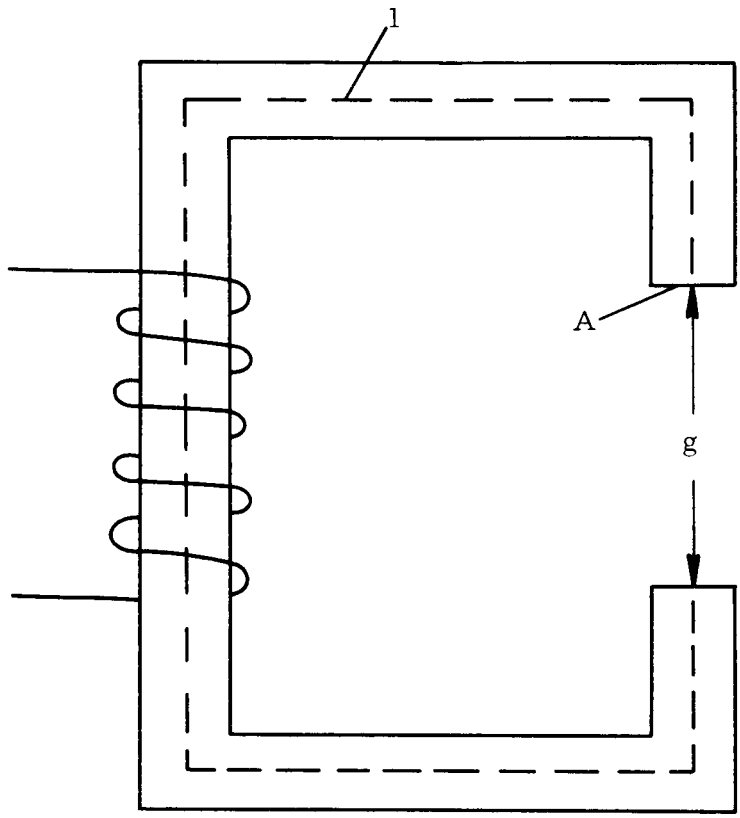

FIG. 17 RELUCTANCE PATH IN "C" CORE ELECTROMAGNET

The above expression permits the reluctance drop in the magnetic portion of the circuit to be neglected.

The maximum allowable exciting current for the electromagnet was determined to be twenty amperes. This would yield a magnetomotance of 9,780 ampere-turns.

$$\mathcal{M} = nI \quad \text{ampere-turns} \tag{10}$$

The magnetomotance is related to the magnetic potential gradient through Weber's Law expressed as

$$\oint H \, d\ell = nI \tag{11}$$

where the integral is taken over the path ℓ + g in Figure 17. In many applications, it is sufficient to calculate an average magnetic field intensity. By relaxing the mathematics, an average gradient can be approximated by the following expression:

$$H \approx \frac{\mathcal{M}}{g}$$

In Figure 5, g is shown to be 4.7 centimeters. The space permeability of a vacuum has been determined to be a constant equal to $4\pi \times 10^{-7}$. The resulting magnetic field intensity is 208 kiloampere-turns per meter. And equation (12) predicted a magnetic field intensity of 261 milliwebers per meter squared.

$$B = \mu_v \mu_a H \tag{12}$$

To resolve an expected output from the electromagnetic flowmeter, a flow velocity had to be determined. The mean flow was to be 110 gallons per minute, therefore an average velocity at this flow rate was determined from equations (13) and (14). To calculate the area perpendicular to fluid flow, the inside diameter of the tube in Figure 6 is is 3.8 centimeters.

$$Q = VA \tag{13}$$

$$A = \frac{\pi d_t^2}{4} \tag{14}$$

where: $Q \triangleq$ volume per unit time
$V \triangleq$ average velocity
$A \triangleq$ total area normal to flow
$d_t \triangleq$ inside diameter of tube

The average velocity was approximately 610 centimeters per second, and using equation (5), the output of the electromagnetic flow transducing device was calculated to be α60.5 milivolts.

REFERENCES

1. Balling, N. R.; and Conner, B. V.: An Electromagnetic Flowmeter for Low Conductivity Fluids. Technical Report No. 32-329, Jet Propulsion Laboratory; Pasadena, California; August 30, 1962.

2. Laue, E. G.: Application of the Electromagnetic Flowmeter to the Testing of Liquid-Propellant Rocket Motors. Memorandum No. 20-109, Jet Propulsion Laboratory; Pasadena, California; March 15, 1955.

BIBLIOGRAPHY

* Doebelin, E. O.: Measurement Systems Application and Design. McGraw-Hill Book Company; pp. 479-484; 1966.

* Muller, G. V.: Introduction to Electrical Engineering. McGraw-Hill Book Company; pp. 198-226; 1957.

* Nussbaum, A.: Magnetic Theory on a Macroscopic Basis. Electronic Design News; pp. 78-88; July 1966.

* Binder, R. C.: Fluid Mechanics. Prentice-Hall, Inc.; pp. 107-134; 1955.

* Cushing, V.: Electromagnetic Flowmeter. The Review of Scientific Instruments; Vol. 36, No. 8; pp. 1142-1148; August 1965.

Cowley, M. D.: Flowmetering by a Motion-induced Magnetic Field. Journal of Scientific Instruments; Vol. 42, pp. 406-409; June 1965.

Cushing, V.; Reily, D.; and Schein, T. R.: Induction Flowmeter for Dielectric Fluids. Engineering-Physics Company; Rockville, Maryland; Contract NASr-53; April 16, 1962.

---

* These publications are of special significance to the discussion in the text.

AN APPLICATION OF THE ELECTROMAGNETIC FLOWMETER FOR ANALYZING DYNAMIC FLOW OSCILLATIONS

By Houston M. Hammac

The information in this report has been reviewed for security classification. Review of any information concerning Department of Defense or Atomic Energy Commission programs has been made by the MSFC Security Classification Officer. This report, in its entirety, has been determined to be unclassified.

This document has also been reviewed and approved for technical accuracy.

E. J. DROST
Chief, Measuring Section

R. R. HEAD
Chief Applied Mechanical Research Branch

H. G. PAUL
Chief, Propulsion Division

W. R. LUCAS
Director, Propulsion and Vehicle Engineering Laboratory

DISTRIBUTION

R-DIR
R-ASTRO-DIR
R-ME-DIR
R-QUAL-DIR
R-RP-DIR
R-TEST-DIR
R-TEST-S
R-TEST-T
R-P&VE-DIR
R-P&VE-M
R-P&VE-S
R-P&VE-V
R-P&VE-P
R-P&VE-P
R-P&VE-PA
R-P&VE-PE
R-P&VE-PM
R-P&VE-PP
R-P&VE-PT
R-P&VE-RT
MS-I
MS-H
K-DIR
MS-T (5)
CC-P
HME-P

Mr. Weidner
Dr. Haeussermann
Mr. Kuers
Mr. Grau
Dr. Stuhlinger
Mr. Heimburg
Mr. Perry
Mr. Sieber
Dr. Lucas
Mr. Kingsbury
Mr. Kroll
Mr. Aberg
Mr. Paul
Mr. Isbell
Mr. Thomson
Dr. Head (25)
Mr. Fuhrmann
Mr. McKay
Mr. Wood
Mr. Hofues
Mr. Remer
Mr. Akens
Dr. Debus

Scientific and Technical Information Facility (25)
Attn: NASA Representative (S-AK/RKT)
P. O. Box 33
College Park, Maryland 20740

Defense Documentation Center (20)
Cameron Station
Alexandria, Virginia 22314